Endothelial cell Nrf2 controls neuroinflammation following a systemic insult

Haoyu Zou[1,2], Zhuochun Huang[1,2], Tom Leah[1,2], Xin He[1,2,3], Owen Dando[1,2,3] & Jing Qiu[1,2]*

[1]UK Dementia Research Institute at The University of Edinburgh, Edinburgh Medical School, 47 Little France Crescent, Edinburgh EH16 4TJ, UK

[2]Centre for Discovery Brain Sciences and [3]Simons Initiative for the Developing Brain, Deanery of Biomedical Sciences, Edinburgh Medical School, University of Edinburgh, Edinburgh, EH8 9XD, UK.

*Correspondence to Jing Qiu Jing.Qiu@ed.ac.uk

Summary

Systemic inflammation can lead to neuroinflammation with acute consequences such as delirium and long-lasting deleterious effects including cognitive decline and the exacerbation of neurodegenerative disease progression. Here we show that the activation status of the transcription factor Nrf2 in endothelial cells is a critical regulator of this process. We found that peripheral inflammation caused infiltration of macrophages, microglial activation and inflammatory reactive astrogliosis, all of which could be prevented by RTA-404, an activator of the transcription factor Nrf2 and close structural relative of the recently FDA-approved Nrf2 activator RTA-408 (Omaveloxolone). To identify the key cellular mediator(s), we generated an endothelial cell-specific Nrf2 knockout mouse. Strikingly, the effects of RTA-404 on brain endothelial activation and downstream neuroinflammatory events was abolished by endothelial cell-specific Nrf2 deletion. This places endothelial cell Nrf2 as a peripherally accessible therapeutic target to reduce the CNS-adverse consequences of systemic inflammation.

Introduction

Systemic inflammation is a major cause of neuroinflammation, key markers of which include infiltration of circulating leukocytes into the brain parenchyma across a compromised blood brain barrier (BBB), as well as microglial activation and inflammatory reactive astrogliosis[1,2,3,4,5,6]. Neuroinflammation can lead acutely to delirium, and chronically to exacerbation of neurodegenerative disease progression including vascular dementia and

Alzheimer's disease[7,8,9,10,11]. Strategies to prevent CNS-adverse consequences of systemic inflammation require a better knowledge of the key pathways that maintain the immune-privileged status of the CNS. Brain endothelial cells (BECs) are an integral component of the BBB, and therefore an attractive proposition as a target for immune system-to-brain signaling[12,13,14].

The transcription factor Nrf2 (encoded by the *Nfe2l2* gene) is a widely-expressed stress-responsive master regulator of genes involved in important aspects of homeostatic physiology including the prevention of redox, metabolic and inflammatory deregulation[15,16,17]. Under normal conditions Nrf2 is targeted for ubiquitin-mediated degradation by Keap1, but in response to stress, this interaction is inhibited, leading to Nrf2 accumulation in the nucleus where it regulates the expression of genes that contain antioxidant response elements (AREs) in their promoter[15,16]. The Nrf2 pathway is pharmacologically activatable via small molecule disruption of Nrf2/Keap1 interactions[15,16]. A potent Nrf2 activator RTA-408 (Omaveloxolone) was recently approved by the FDA for treating Friedreich's Ataxia, a genetic neurodegenerative disease associated with oxidative stress[18,19]. This provides proof-of-concept that Nrf2 can be safely activated in humans. In the brain, Nrf2 is highly expressed in BECs, microglia and astrocytes, with low expression in neurons[20]. However, cell-type specific roles of Nrf2 are not well understood, partly due to a historical reliance on global Nrf2 knockout mice to probe the roles of Nrf2[21]. This knowledge gap is important to fill because cell type-specific roles of Nrf2 are likely to be influenced by the function of that cell type, and from a translational point of view one ideally needs to know the locus of action of any Nrf2-targeting therapeutic in order to optimise bioavailability. In this study, we hypothesised that EC Nrf2 specifically plays a role in regulating trans-BBB inflammatory signalling.

Results

Nrf2 activator RTA-404 promotes brain endothelial barrier strength

RTA-404 is a potent Nrf2 activator and close structural relative of RTA-408, with a wide therapeutic window, unlike some electrophilic Nrf2 activators[22]. Previously, our work has focussed on the impact of RTA-404 on astrocytes[23]. We demonstrated that in vitro RTA-404 triggers a neuro-protective response in astrocytes via a Nrf2-dependent transcriptional programme[23]. However, the effects of RTA-404 on BECs were unknown. To test this, we treated

BEC cultures with RTA-404, observing the expected activation of Nrf2 as assessed by studying expression of the prototypical Nrf2 target gene *Hmox1* (Fig. 1A). In vitro, BEC barrier strength can be assessed by measuring trans-endothelial electrical resistance (TEER). We found that RTA-404 caused an increase in BEC TEER in a dose-dependent manner (Fig. 1B and C). Thus, BEC Nrf2 activation by RTA-404 has the potential to promote barrier integrity, begging the question as to whether similar effects can be observed in vivo.

Nrf2 activator RTA-404 modifies the BEC transcriptome under inflammatory conditions

It is well established that systemic inflammation can lead to BBB compromise and neuroinflammation, so we employed a model of systemic inflammation to determine whether pharmacologically activating Nrf2 with RTA-404 can modify neuroinflammation. We induced systemic inflammation in mice by intraperitoneal injection of bacterial endotoxin LPS in *Nfe2l2*$^{LoxP/LoxP}$ mice, chosen as a "conditional-ready" control to compare with conditional knockout mice used later in the study. BECs were sorted by FACS 24h post-LPS and RNA-seq performed, revealing a widespread inflammatory response (Fig. 2A). Pre-administration of RTA-404 significantly modulated the BEC transcriptome under conditions of LPS exposure (Fig. 2B). Known Nrf2 target genes, including several glutathione S-transferases (e.g. *Gsta4* and *Gstp1*), were induced, and a significant number of genes were down-regulated (142 down-regulated and 92 up-regulated genes (*DESeq2 P*_adj<0.05; Fig.2B). Ingenuity Pathway Analysis (IPA) of genes significantly altered by RTA-404 revealed several down-regulated signatures associated with inflammation, particularly interferon signalling (Fig. 2C). Thus, RTA-404 significantly modifies the BEC transcriptome following an inflammatory insult.

Endothelial cell-specific knockout of Nrf2 abolishes the effect of RTA-404 on the BEC transcriptome under inflammatory conditions

We next wanted to investigate the site of action of RTA-404 with respect to its influence on the BEC transcriptome under conditions of LPS treatment, since the effect of RTA-404 could be due to direct activation of BEC Nrf2 or due to indirect effects of RTA-404 on the immune system response to LPS injection (intraperitoneal injection of LPS activates tissue-resident macrophages there as well as inducing inflammatory responses in circulating immune cells[4]). We first investigated the role of Nrf2 in the BECs themselves. We used *Nefe2l2*$^{fl/fl}$ mice which possess *loxP* sites on either side of exon 5 of the *Nefe2l2* gene that encodes the DNA binding

domain Nrf2 protein. *Nefe2l2*$^{fl/fl}$ mice were crossed onto a line, *Cdh5*^{CreERT28} which expresses tamoxifen-inducible CreERT specifically in endothelial cells, to generate an inducible-conditional EC-specific knockout line (*Cdh5*^{CreERT2}*:Nfe2l2*$^{fl/fl}$, hereafter *Nfe2l2*^{ENDO}). Sorting of brain cells by FACS followed by qPCR confirmed successful deletion of Nrf2 exon 5 in BECs, without affecting Nrf2 levels in astrocytes, microglia or oligodendrocytes (Fig. 3A). As expected, Nrf2-deficient BECs exhibited a down-regulation of several known Nrf2 target genes (e.g. *Txnrd1* and *Gstm1*, Fig. 3B), although the modest magnitude of changes observed suggested that basal Nrf2 activity in BECs is relatively low. We next assessed the influence of RTA-404 on the BEC transcriptome of *Nfe2l2*^{ENDO} mice under conditions of LPS exposure. In contrast to the influence of RTA-404 on *Nfe2l2*$^{fl/fl}$ BECs, the effect of RTA-404 was essentially abolished in *Nfe2l2*^{ENDO} BECs (Fig. 3C). This strongly suggests that BEC Nrf2 is the locus of action for RTA-404, as opposed to upstream events such as LPS-induced immune cell activation.

Endothelial cell Nrf2 maintains microglial homeostatic signature and regulates microglial activation under inflammatory conditions

Neuroinflammation following a peripheral inflammatory insult is characterised by microglial activation and reactive astrogliosis, and can involve infiltration of circulating immune cells, such as macrophages, into the brain parenchyma[4]. As expected, microglia and astrocytes display widespread transcriptional changes following LPS exposure (Fig. 4 A & Fig. 5A). Pre-administration of RTA-404 significantly modulated the transcriptome of microglia under conditions of LPS exposure (Fig. 4B). Of note, microglial homeostatic signature genes (MHSGs) such as *Tmem119*, *Sparc*, *Tgfbr1*, and *P2ry12* were significantly upregulated (Fig. 4B). To assess this systematically we took the set of MHSGs defined by Butovsky et al. (2014)[27] and looked at the influence of pre-administration of RTA-404 on the expression of MHSGs under conditions of LPS exposure. Expression of these genes were significantly upregulated by pre-administration of RTA-404 under conditions of LPS exposure (Fig.4D), suggesting that pharmacologically activating Nrf2 has the capacity to maintain MHSG expression under inflammatory conditions. IPA analysis of genes significantly altered by RTA-404 in microglia revealed several down-regulated signatures associated with inflammation, particularly interleukin signalling, cell surface interactions at the vascular wall and leukocyte extravasation signalling (Fig. 4E). To further assess whether RTA-404 had the capacity to modulate microglial responses to LPS, we took microglial genes up- and down-regulated by LPS and studied the

impact of RTA-404 pre-treatment. We found that the gene set induced by LPS in microglia was overall repressed by RTA-404 treatment (Fig. 4F (i & iii)), and the gene set repressed by LPS in microglia was overall elevated by RTA-404 treatment (Fig. 4G (i & iii)). Thus, RTA-404 was successful in suppressing microglial responses to peripheral LPS administration. We next asked whether the influence of RTA-404 on the microglial response involved activation of Nrf2 in ECs. Notably, when we performed the experiment on *Nfe2l2*^{ENDO} mice we found that the effect of RTA-404 on the microglial transcriptome was abolished (Fig. 4C). In addition, cross-reference analysis showed that no significant effect of RTA-404 was observed on LPS-induced changes in microglia (Fig. 4F (ii & iii) & Fig. 4G (ii & iii)). Thus, the impact of RTA-404 on microglia's inflammatory response to peripheral LPS administration is mediated by EC Nrf2 activation.

Endothelial cell Nrf2 regulates astrogliosis under inflammatory conditions

We next analysed astrocytes sorted from LPS-treated *Nfe2l2*$^{fl/fl}$ and *Nfe2l2*^{ENDO} mice. As with microglia, pre-administration of RTA-404 significantly modulated the transcriptome of astrocytes under conditions of LPS exposure (Fig. 5B). Of note, the expression of classic astrogliosis marker *Gfap* was downregulated by RTA-404 under LPS exposure (Fig. 5B). IPA pathway analysis shows of genes significantly altered by RTA-404 in astrocytes revealed down-regulated signatures associated with inflammation, particularly interferon signalling and interleukin signalling (Fig. 5D). Like in microglia, we observed an RTA-404-induced suppression of LPS-induced inflammatory responses in astrocytes: RTA-404 significantly inhibited the set of LPS-activated genes (Fig. 5C (i & iii)), and up-regulated the set of LPS-repressed genes (Fig. 5D (i & iii)). Moreover, the effect of RTA-404 on the astrocyte transcriptome under conditions of LPS exposure was abolished in *Nfe2l2*^{ENDO} mice (Fig. 5C) and no significant effect of RTA-404 was observed on LPS-induced changes in astrocytes (Fig. 5E (ii & iii) & Fig. 5F (ii & iii)). Thus, despite the theoretical ability of RTA-404 to activate Nrf2 directly in microglia and astrocytes, the effects of RTA-404 on these cell types are in fact mediated by Nrf2 in endothelial cells.

Endothelial cell Nrf2 regulates immune cell brain infiltration under inflammatory conditions

Neuroinflammation due to a peripheral insult can involve infiltration of circulating immune cells via a compromised BBB[4]. Since our observation that RTA-404 strengthened the TEER of a BEC monolayer in vitro, we wanted to assess whether RTA-404 could prevent BBB compromise. In our model of i.p. LPS administration we observe substantial peripheral

macrophage infiltration into the brain parenchyma, assessed by flow cytometry, where $CD11b^{+}CD45^{low}$ microglia and $CD11b^{+}CD45^{high}$ macrophages can be distinguished. To confirm the gating strategy for brain microglia and macrophage populations in flow cytometry analysis, we took advantage of *Csf1r*$^{\Delta FIRE/\Delta FIRE}$ mice in which brain microglia are lacking but other macrophage populations are unaffected (Fig. S1B). We observed parenchymal infiltration of $CD11b^{+}CD45^{high}$ macrophages upon peripheral LPS administration (Fig. 6A (i & ii) and Fig.6B) in *Nfe2l2*$^{fl/fl}$ mice. Importantly, RTA-404 administration abolished macrophage infiltration into the brain (Fig. 6A (iii) and Fig. 6B). Strikingly, the effect of RTA-404 in preventing macrophage infiltration into the parenchyma was abolished in *Nfe2l2*^{ENDO} mice (Fig.6A (vi) and Fig.6B). Thus, EC Nrf2 can play a key role in preventing immune cell infiltration into the brain parenchyma following peripheral inflammation.

Discussion

Overall, our study identifies Nrf2 specifically in ECs regulates immune system-to-brain communication. The mechanisms by which Nrf2 activation suppress neuroinflammation may involve a combination of supressing EC inflammatory responses (e.g. EC chemokine release) as well as maintaining BBB integrity to prevent immune cell infiltration into the brain parenchyma. As such, BEC Nrf2 may play a classical anti-inflammatory role, but also a cell-type specific roles such as regulation of barrier integrity. Indeed, tight junction protein Jam3[26] is up-regulated by RTA-404 treatment in BECs and down-regulated by Nrf2 KO in BECs. However, further investigations are needed to define the precise mechanism behind EC Nrf2-dependent prevention of immune cell infiltration.

As well as providing a greater understanding of the cell type-specific roles of Nrf2, our work suggests that EC Nrf2 is a tractable therapeutic target for neuroinflammation, with the advantage of being a CNS-relevant target that can be targeted by non-CNS-penetrating drugs. The growing appreciation of the long-lasting impact of immune system-to-brain signalling on cognitive function and neurodegenerative disease trajectory makes it essential to develop strategies to combat this[24,25]. The positive impact of RTA-404 in limiting neuroinflammation, coupled with the recent clinical success of its close relative RTA-408, suggest that administration of these or similar compounds may limit the CNS-adverse effects of peripheral inflammation. The effect of RTA-404 is striking, as is the fact that its effects are abolished in

endothelial cell-specific Nrf2 deficient mice. We cannot rule out that RTA-404 is influencing events upstream of BECs (peripheral ECs) or downstream events (e.g. microglial and astrocyte responses). However, the striking abolition of the effects of RTA-404 in *Nfe2l2*^{ENDO} mice point to EC Nrf2 being necessary. We conclude that EC Nrf2 acts as a gatekeeper of BBB integrity and neuroinflammation and is potentially a promising therapeutic target for preventing systemic inflammation induced neuroinflammation in a range of clinical settings.

Limitations of the study

One limitation of this study is that our genetic strategy employed to knock-out NRF2 does so in all ECs. An alternative strategy would be needed to be knock out NRF2 in BECs only in order to definitively implicate BEC NRF2 as a gatekeeper of neuroinflammation. While a mouse line has been generated that expresses Cre-ERT2 in BECs and no other ECs (*Slco1c1*-CreER^{T2} mice[29]) it also is expressed in a proportion of astrocytes[29] which would be problematic for us given the high level of expression and functional importance of astrocytic NRF2[30]. The other limitation of the study is that while we show EC NRF2 to be *necessary* for the effect of RTA-404 on neuroinflammation, we don't show that EC NRF2 is sufficient to prevent neuroinflammation following a peripheral insult. This would likely require EC or BEC-specific over-expression of NRF2 by generating a new transgenic mouse or EC-targeted AAVs (such as AAV9-X1[31]). Such gain-of-function experiments are part of our ongoing plans.

STAR★Methods

Key Resources Table

REAGENTS or RESOURCE	RESOURCE	IDENTIFIER
Antibodies		
PE/Cyanine7 anti-mouse CD31	Biolegend	Cat #102523; RRID: AB_2572181
FITC anti-mouse CD11b	Biolegend	Cat #101206; RRID: AB_312788
BV anti-ly6G	Biolegend	Cat #127643; RRID: AB_AB_2565971
PE anti-mouse/human/rat O4	Miltenyibiotec	Cat #130-117-357
APC anti-mouse/human/rat ACSA2	Miltenyibiotec	Cat #130-116-142
Chemicals		
Tamoxifen (TAM)	Merck Life Sciences UK	Cat #T5648
Corn oil	Merck Life Sciences UK	Cat #C8267
LPS from *Escherichia coli* O111:B4	InvivoGen	Cat # tlrl-3pelps
Bovine serum albumin (BSA)	Merck Life Sciences UK	Cat #A9647
RNAprotect Cell Reagent	Qiagen	Cat #76526
CDDO-TFEA	Cambridge Bioscience LTD	Cat #90001845-10mg-CAY
Critical Commercial Assays		
RNeasy Plus Micro Kit	Qiagen	Cat #74034
Adult Brain Dissociation Kit	Miltenyibiotec	Cat #130-107-677
MERCURIUS™ DRUG-seq library preparation kit	Alithea Genomics SA	Cat #10841
Deposited Data		
RNA-seq data sets	European Bioinformatics Institute-ArrayExpress	E-MTAB-14404
Experimental Models: Mouse Strains		
$Nrf2^{flox}$ mouse line	Kong et al., 2011	The Jackson Laboratory stock#25433
$CDH5^{CreERT2}$ mouse line	Wang et al., 2010	N/A
Oligonucleotides		
Gapdh Fwd primer 5'-GGGTGTGAACCACGAGAAAT-3'	Merck Life Sciences UK	Custom
Gapdh Rev primer 5'-CCTTCCACAATGCCAAAGTT-3'	Merck Life Sciences UK	Custom
Nefe2l2 exon5 Fwd primer 5'-TCCATTTACGGAGACCCACC-3'	Merck Life Sciences UK	Custom
Nefe2l2 exon5 Rev primer 5'-GGATTCACGCATAGGAGCAC-3'	Merck Life Sciences UK	Custom
Software and Algorithm		
Prism	GraphPad	https://www.graphpad.com/scientific-software/prism/
FCS Express	De Novo Software	https://denovosoftware.com
Ingenuity Pathway Analysis	Qiagen	N/A

Resource availability

Lead Contact

Further information and requests for resources and reagents should be directed to and will be fulfilled by the Lead Contact, Jing Qiu (jing.qiu@ed.ac.uk).

Materials Availability

This study did not generate new unique reagents.

Data and Code Availability

All RNA-seq data that support the findings of this study is available at the European Bioinformatics Institute (ArrayExpress: E-MTAB-14404). All other data are available from the lead contact upon reasonable request.

Experimental Model and Subject Details

Mice

The animals involved in this study were all on C57BL/6 background. The CDH5^{CreERT2} mouse line was originally developed in the laboratory of Dr. Ralf Adams[28] and kindly provided by Prof. Andy Baker of University of Edinburgh. The Nrf2^{flox} mouse line was originally generated in the laboratory of Dr. Shyam Biswal and imported from Jackson Laboratories (Mouse Strain Number – 025433). The Nrf2^{flox} mice carrying *loxP* sites flanking exon 5 of the *Nfe2l2* gene were crossed to the CDH5^{CreERT2} mouse line[28] to generate *Cdh5^{CreERT2}: Nefe2l2$^{fl/fl}$* mice. Male mice have been used throughout the study. All procedures described were performed at the University of Edinburgh in compliance with the UK Animals (Scientific Procedures) Act 1986 and University of Edinburgh regulations and carried out under project license numbers P2262369. Mice were group-housed in environmentally enriched cages within humidity and temperature-controlled rooms, with a 12-h light dark cycle with free access to food and water. Mouse genotypes were determined using real-time PCR with transgene specific probes (Transnetyx, Cordova, TN) unless otherwise stated.

Method Details

Tamoxifen, RTA-404 and LPS Treatments

For induction of Cre recombinase activity, 6-8-week-old *Cdh5^{CreERT2}: Nefe2l2$^{fl/fl}$* mice were given orally with 8 mg tamoxifen (TAM, T5648, Sigma-Aldrich, UK) solved in corn oil (C8267, Sigma-Aldrich, UK) at 4 time points with 24hrs apart. For all experiments, littermates carrying the respective loxP-flanked alles but lacking expression of Cre recombinase (+/+ TAM) were used as controls. Male mice have been used throughout the study. The *Cdh5^{CreERT2}: Nefe2l2$^{fl/fl}$* mice and control mice were injected peritoneally with 5mg/kg of RTA-404 (90001845-10mg-CAY, CAMBRIDGE BIOSCIENCE LTD, UK) for 4 consecutive days with 24 hrs apart, following which 3mg/kg of LPS (tlrl-3pelps, Invivogen, US) was given intraperitoneally to the mice for 24 hrs.

Isolation of brain cells, Cell Sorting, and RNA extraction

Single brain cells were isolated using Adult Brain Dissociation kit (Miltenyie, 130-107-677, Germany) as per the manufacturer's instructions. The single brain cell suspension was then

incubated with antibodies against CD31 (Biolegend, 102523, UK) CD11b (Biolegend, 101205, UK), ACSA2 (Miltenyie, 130-116-245, Germany), O4 (Miltenyie, 130-117-357, Germany), CD45 (Biolegend, 103125, Germany) for 15 minutes in ice, washed with PBS and then immediately FACS sorted into RNAprotect Cell Reagent (Qiagen, 76526, UK) under the gates of $CD31^{+}CD45^{-}$ $ACSA2^{-}$ for BECs, $LY6G^{-}CD11b^{+}CD45^{low}$ for microglia, $ACSA^{+}O4^{-}$ for astrocytes and $O4^{+}$ for oligodendrocytes (Fig. S1). RNA extraction was carried out using the RNeasy Plus Micro Kit (Qiagen) as per the manufacturer's instructions.

Quantitative RT-PCR

cDNA was generated using the Transcriptor First Strand cDNA Synthesis Kit (Roche). Seven microlitres of RNA was added to the RT and buffer mixture prepared with random hexamers and oligoDT primers as per kit instructions, and qRT-PCR carried out with the following programme: 10 min at 25 °C, 30 min at 55 °C and 5 min at 85 °C. qPCRs were run on a Stratagene Mx3000P QPCR System (Agilent Technologies) using SYBR Green MasterRox (Roche) with 6 ng of cDNA per well of a 96-well plate, using the following programme: 10 min at 95 °C, 40 cycles of 30 s at 95 °C, 40 s at 60 °C and 30 s at 72 °C, with a subsequent cycle of 1 min at 95 °C and 30 s at 55 °C ramping up to 95 °C over 30 s (to measure the dissociation curve).

RNA-seq and Analysis

For standard TruSeq (Experiments presented in Figures 2A, 3B, 4A, and 5A), libraries were prepared by Edinburgh Genomics using the Illumina TruSeq stranded mRNA-seq kit, according to the manufacturer's protocol (Illumina). The libraries were pooled and sequenced to 75 base paired-end on an Illumina NovaSeqTM 6000 to a depth of approximately 50 million paired-end reads per sample. For barcoded mRNA sequencing (Experiments presented in Figures 2B, 3C, 4B & C, 5B & C), RNA sequencing libraries were prepared using the MERCURIUS Drug-seq v2 library Preparation 96 kit as per the manufacturer's instructions. Briefly, each RNA sample was reverse transcribed in a 96-well plate with individual barcoded oligo-dT primers. Next, all the samples were pooled together, purified using the DNA Clean and Concentrator kit (Zymo Research, Cat.#D4014), and treated with exonuclease I. Double-stranded cDNA was generated by the second stand synthesis via the nick translation method. Full-length double-stranded cDNA was purified with 30 µL (0.6x) of AMPure XP magnetic

beads (Beckman Coulter, Cat.#A63881) and eluted in 20 µL of water. The Illumina compatible libraries were prepared by tagmentation of 5 ng of full-length double-stranded cDNA with 1 µL of in-house produced Tn5 enzyme (11 µM). The final library was amplified using 15 cycles and the fragments ranging 200–1000 bp were size-selected using AMPure beads (Beckman Coulter, Cat.#A63881) (first round 0.5x beads, second 0.7x). The libraries were profiled with the High Sensitivity NGS Fragment Analysis Kit (Advanced Analytical, Cat.#DNF-474) and measured with the Qubit dsDNA HS Assay Kit (Invitrogen, Cat.#Q32851) prior to pooling and sequencing using the Illumina NextSeq 2000 P2 platform. For read mapping and feature counting, genome sequences and gene annotations were downloaded from Ensembl version 94. Differential expression (DGE) analysis on data sets was performed using DESeq2 (R package version 1.18.1) using a significance threshold set at a Benjamini-Hochberg-adjusted p-value of 0.05.

Acknowledgements

We would like to thank the Flow Cytometry Facility, led by Dr. Fiona Rossi, at the Centre for Regenerative Medicine at the University of Edinburgh for their help with the Flow Cytometry work. The research leading to these results received funding from the Ann Rowling Regenerative Neurology Clinic at the University of Edinburgh.

Author contributions

H.Z., Z.H. and T.L. performed the experiments. X.H., O.D., H.Z., and J.Q. analysed the data. J.Q. conceived the study and wrote the manuscript.

Declaration of interests

The authors declare no competing interests.

References

1. Perry VH. Contribution of systemic inflammation to chronic neurodegeneration. Acta Neuropathol. 2010 Sep;120(3):277-86. doi: 10.1007/s00401-010-0722-x. Epub 2010 Jul 20. PMID: 20644946.
2. Gao Q, Hernandes MS. Sepsis-Associated Encephalopathy and Blood-Brain Barrier Dysfunction. Inflammation. 2021 Dec;44(6):2143-2150. doi: 10.1007/s10753-021-01501-3. Epub 2021 Jul 21. PMID: 34291398; PMCID: PMC11044530.

3. Sun Y, Koyama Y, Shimada S. Inflammation From Peripheral Organs to the Brain: How Does Systemic Inflammation Cause Neuroinflammation? Front Aging Neurosci. 2022 Jun 16;14:903455. doi: 10.3389/fnagi.2022.903455. PMID: 35783147; PMCID: PMC9244793.
4. Xingi E, Koutsoudaki PN, Thanou I, Phan MS, Margariti M, Scheller A, Tinevez JY, Kirchhoff F, Thomaidou D. LPS-Induced Systemic Inflammation Affects the Dynamic Interactions of Astrocytes and Microglia with the Vasculature of the Mouse Brain Cortex. Cells. 2023 May 17;12(10):1418. doi: 10.3390/cells12101418. PMID: 37408252; PMCID: PMC10217139.
5. Millán Solano MV, Salinas Lara C, Sánchez-Garibay C, Soto-Rojas LO, Escobedo-Ávila I, Tena-Suck ML, Ortíz-Butrón R, Choreño-Parra JA, Romero-López JP, Meléndez Camargo ME. Effect of Systemic Inflammation in the CNS: A Silent History of Neuronal Damage. Int J Mol Sci. 2023 Jul 25;24(15):11902. doi: 10.3390/ijms241511902. PMID: 37569277; PMCID: PMC10419139.
6. Xin Y, Tian M, Deng S, Li J, Yang M, Gao J, Pei X, Wang Y, Tan J, Zhao F, Gao Y, Gong Y. The Key Drivers of Brain Injury by Systemic Inflammatory Responses after Sepsis: Microglia and Neuroinflammation. Mol Neurobiol. 2023 Mar;60(3):1369-1390. doi: 10.1007/s12035-022-03148-z. Epub 2022 Nov 29. PMID: 36445634; PMCID: PMC9899199.
7. Cunningham C. Systemic inflammation and delirium: important co-factors in the progression of dementia. Biochem Soc Trans. 2011 Aug;39(4):945-53. doi: 10.1042/BST0390945. PMID: 21787328; PMCID: PMC4157218.
8. Lim SL, Rodriguez-Ortiz CJ, Kitazawa M. Infection, systemic inflammation, and Alzheimer's disease. Microbes Infect. 2015 Aug;17(8):549-56. doi: 10.1016/j.micinf.2015.04.004. Epub 2015 Apr 22. PMID: 25912134.
9. Sipilä PN, Heikkilä N, Lindbohm JV, Hakulinen C, Vahtera J, Elovainio M, Suominen S, Väänänen A, Koskinen A, Nyberg ST, Pentti J, Strandberg TE, Kivimäki M. Hospital-treated infectious diseases and the risk of dementia: a large, multicohort, observational study with a replication cohort. Lancet Infect Dis. 2021 Nov;21(11):1557-1567. doi: 10.1016/S1473-3099(21)00144-4. Epub 2021 Jun 21. PMID: 34166620; PMCID: PMC8592915.
10. Tian Z, Ji X, Liu J. Neuroinflammation in Vascular Cognitive Impairment and Dementia: Current Evidence, Advances, and Prospects. Int J Mol Sci. 2022 Jun 2;23(11):6224. doi: 10.3390/ijms23116224. PMID: 35682903; PMCID: PMC9181710.
11. Thakur S, Dhapola R, Sarma P, Medhi B, Reddy DH. Neuroinflammation in Alzheimer's Disease: Current Progress in Molecular Signaling and Therapeutics. Inflammation. 2023 Feb;46(1):1-17. doi: 10.1007/s10753-022-01721-1. Epub 2022 Aug 20. PMID: 35986874.
12. Abbott NJ, Friedman A. Overview and introduction: the blood-brain barrier in health and disease. Epilepsia. 2012 Nov;53 Suppl 6(0 6):1-6. doi: 10.1111/j.1528-1167.2012.03696.x. PMID: 23134489; PMCID: PMC3625728.
13. Kadry H, Noorani B, Cucullo L. A blood-brain barrier overview on structure, function, impairment, and biomarkers of integrity. Fluids Barriers CNS. 2020 Nov 18;17(1):69. doi: 10.1186/s12987-020-00230-3. PMID: 33208141; PMCID: PMC7672931.
14. Fang YC, Hsieh YC, Hu CJ, Tu YK. Endothelial Dysfunction in Neurodegenerative Diseases. Int J Mol Sci. 2023 Feb 2;24(3):2909. doi: 10.3390/ijms24032909. PMID: 36769234; PMCID: PMC9918222.
15. Johnson DA, Johnson JA. Nrf2--a therapeutic target for the treatment of neurodegenerative diseases. Free Radic Biol Med. 2015 Nov;88(Pt B):253-267. doi: 10.1016/j.freeradbiomed.2015.07.147. Epub 2015 Aug 14. PMID: 26281945; PMCID: PMC4809057.

16. Tebay LE, Robertson H, Durant ST, Vitale SR, Penning TM, Dinkova-Kostova AT, Hayes JD. Mechanisms of activation of the transcription factor Nrf2 by redox stressors, nutrient cues, and energy status and the pathways through which it attenuates degenerative disease. Free Radic Biol Med. 2015 Nov;88(Pt B):108-146. doi: 10.1016/j.freeradbiomed.2015.06.021. Epub 2015 Jun 27. PMID: 26122708; PMCID: PMC4659505.
17. Abeti R, Baccaro A, Esteras N, Giunti P. Novel Nrf2-Inducer Prevents Mitochondrial Defects and Oxidative Stress in Friedreich's Ataxia Models. Front Cell Neurosci. 2018 Jul 17;12:188. doi: 10.3389/fncel.2018.00188. PMID: 30065630; PMCID: PMC6056642.
18. Murakami S, Kusano Y, Okazaki K, Akaike T, Motohashi H. NRF2 signalling in cytoprotection and metabolism. Br J Pharmacol. 2023 Sep 15. doi: 10.1111/bph.16246. Epub ahead of print. PMID: 37715470.
19. Lee A. Omaveloxolone: First Approval. Drugs. 2023 Jun;83(8):725-729. doi: 10.1007/s40265-023-01874-9. PMID: 37155124.
20. 2024@BRAIN RNA-SEQ https://brainrnaseq.org
21. Pant A, Dasgupta D, Tripathi A, Pyaram K. Beyond Antioxidation: Keap1-Nrf2 in the Development and Effector Functions of Adaptive Immune Cells. Immunohorizons. 2023 Apr 1;7(4):288-298. doi: 10.4049/immunohorizons.2200061. PMID: 37099275; PMCID: PMC10579846.
22. Baxter PS, Márkus NM, Dando O, He X, Al-Mubarak BR, Qiu J, Hardingham GE. Targeted de-repression of neuronal Nrf2 inhibits α-synuclein accumulation. Cell Death Dis. 2021 Feb 26;12(2):218. doi: 10.1038/s41419-021-03507-z. PMID: 33637689; PMCID: PMC7910424.
23. Gupta K, Patani R, Baxter P, Serio A, Story D, Tsujita T, Hayes JD, Pedersen RA, Hardingham GE, Chandran S. Human embryonic stem cell derived astrocytes mediate non-cell-autonomous neuroprotection through endogenous and drug-induced mechanisms. Cell Death Differ. 2012 May;19(5):779-87. doi: 10.1038/cdd.2011.154. Epub 2011 Nov 18. PMID: 22095276; PMCID: PMC3321621.
24. Peralta Ramos JM, Kviatcovsky D, Schwartz M. Targeting the immune system towards novel therapeutic avenues to fight brain aging and neurodegeneration. Eur J Neurosci. 2022 Nov;56(9):5413-5427. doi: 10.1111/ejn.15609. Epub 2022 Feb 19. PMID: 35075702.
25. Passaro AP, Lebos AL, Yao Y, Stice SL. Immune Response in Neurological Pathology: Emerging Role of Central and Peripheral Immune Crosstalk. Front Immunol. 2021 Jun 10;12:676621. doi: 10.3389/fimmu.2021.676621. PMID: 34177918; PMCID: PMC8222736.
26. Akawi NA, Canpolat FE, White SM, Quilis-Esquerra J, Morales Sanchez M, Gamundi MJ, Mochida GH, Walsh CA, Ali BR, Al-Gazali L. Delineation of the clinical, molecular and cellular aspects of novel JAM3 mutations underlying the autosomal recessive hemorrhagic destruction of the brain, subependymal calcification, and congenital cataracts. Hum Mutat. 2013 Mar;34(3):498-505. doi: 10.1002/humu.22263. PMID: 23255084; PMCID: PMC3951164.
27. Butovsky O, Jedrychowski MP, Moore CS, Cialic R, Lanser AJ, Gabriely G, Koeglsperger T, Dake B, Wu PM, Doykan CE, Fanek Z, Liu L, Chen Z, Rothstein JD, Ransohoff RM, Gygi SP, Antel JP, Weiner HL. Identification of a unique TGF-β-dependent molecular and functional signature in microglia. Nat Neurosci. 2014 Jan;17(1):131-43. doi: 10.1038/nn.3599. Epub 2013 Dec 8. Erratum in: Nat Neurosci. 2014 Sep;17(9):1286. PMID: 24316888; PMCID: PMC4066672.
28. Wang Y, Nakayama M, Pitulescu ME, Schmidt TS, Bochenek ML, Sakakibara A, Adams S, Davy A, Deutsch U, Lüthi U, Barberis A, Benjamin LE, Mäkinen T, Nobes CD, Adams RH.

Ephrin-B2 controls VEGF-induced angiogenesis and lymphangiogenesis. Nature. 2010 May 27;465(7297):483-6. doi: 10.1038/nature09002. PMID: 20445537.
29. Ridder DA, Lang MF, Salinin S, Röderer JP, Struss M, Maser-Gluth C, Schwaninger M. TAK1 in brain endothelial cells mediates fever and lethargy. J Exp Med. 2011 Dec 19;208(13):2615-23. doi: 10.1084/jem.20110398. Epub 2011 Dec 5. PMID: 22143887; PMCID: PMC3244031.
30. Johnson DA, Johnson JA. Nrf2--a therapeutic target for the treatment of neurodegenerative diseases. Free Radic Biol Med. 2015 Nov;88(Pt B):253-267. doi: 10.1016/j.freeradbiomed.2015.07.147. Epub 2015 Aug 14. PMID: 26281945; PMCID: PMC4809057.
31. Chen X, Wolfe DA, Bindu DS, Zhang M, Taskin N, Goertsen D, Shay TF, Sullivan EE, Huang SF, Ravindra Kumar S, Arokiaraj CM, Plattner VM, Campos LJ, Mich JK, Monet D, Ngo V, Ding X, Omstead V, Weed N, Bishaw Y, Gore BB, Lein ES, Akrami A, Miller C, Levi BP, Keller A, Ting JT, Fox AS, Eroglu C, Gradinaru V. Functional gene delivery to and across brain vasculature of systemic AAVs with endothelial-specific tropism in rodents and broad tropism in primates. Nat Commun. 2023 Jun 8;14(1):3345. doi: 10.1038/s41467-023-38582-7. PMID: 37291094; PMCID: PMC10250345

Figure Legends

Fig.1. Nrf2 activator RTA-404 promotes brain endothelial barrier strength

(A) Human BEC cultures were treated with ±RTA-404 for 24h, RNA was extracted and *Hmox1* analyzed by qRT-PCR, normalized to *GAPDH*. *p=0.0326, One-way ANOVA plus Sidak post hoc (n=4).

(B) Human BEC cultures were treated with ±RTA-404 and transepithelial/transendothelial electrical resistance (TEER) was measured for 20 hrs. *p<0.0001, Two-way ANOVA (n=8-9).

(C) Changes in TEER in human BEC culture at 20 hrs post-treatment with RTA-404 at 100nM, 200nM and 400nM respectively compared to that in the saline control group, *p=0.0136, One-way ANOVA plus Sidak post hoc (n=8-9).

Fig.2. Nrf2 activator RTA-404 modifies the BEC transcriptome under inflammatory conditions

Mice were given i.p. injection of either saline or RTA-404 (n=6-8) daily for 4 days, following which either saline or LPS was given for 24 hrs. The brain cells were isolated and then sorted with FACS for BECs, RNA extracted and RNA-seq performed. Scatterplot was generated for genes with average expression >0.1 FPKM across the data sets. Highlighted with red and blue crosses are the genes whose expression are significantly increased or decreased respectively (*DESeq2 P*_adj<0.05, n=6-8). 'N' refers here and throughout as an independent replicate (i.e. a mouse).

(A) Scatterplot of RNA-seq analysis showing the BEC transcriptome modified by peripheral LPS insult compared with saline in *Nfe2l2*$^{fl/fl}$ mice (LPS vs Saline).

(B) Scatterplot of RNA-seq analysis showing the LPS-induced BEC transcriptome modified by pre-administration of RTA-404 in *Nfe2l2*$^{fl/fl}$ mice (LPS+RTA-404 vs. LPS+saline).

(C) IPA analysis identifying activated or inhibited pathways by pre-administration of RTA-404 under conditions of LPS exposure (LPS+RTA-404 vs. LPS+saline). Significantly DEGs (*DESeq2 P*_adj<0.05, $|Log_2FC|$>1, n=6-8) with BEC transcriptome as reference dataset were analyzed to calculate the p-value of overlap and z-score of overall activation/inhibition states of individual pathways. The significant activated (p<0.05, z-score >2) or inhibited (p<0.05, z-score<-2) pathways are shown in the bar chart in orange and blue respectively.

Fig.3. Endothelial cell-specific knockout of Nrf2 abolishes the effect of RTA-404 on the BEC transcriptome under inflammatory conditions

(A) qRT-PCR confirms gene expression of exon 5 of Nrf2 is specifically deleted in BECs, but not in astrocytes, microglia or oligodendrocytes in *Nfe2l2*^{ENDO} mice. From left to right p=0.0007, 0.0995, 0.6903, and 0.7432, n=4, unpaired t-test.

(B) Scatterplot of RNA-seq analysis showing the influence of Nrf2 specific KO in BECs on BEC transcriptome at basal condition. Two weeks after tamoxifen-induced recombination, BECs were FCAS sorted from *Nfe2l2*^{ENDO} mice and their *Nfe2l2*$^{fl/fl}$ littermate's control mice. Scatterplot was generated for genes with average expression >0.1 FPKM across the data sets. Highlighted with red and blue crosses are the genes whose expression are significantly increased or decreased respectively (*DESeq2 P*_adj<0.05, n=4-6).

(C) Scatterplot of RNA-seq analysis showing the LPS-induced BEC transcriptome modified by pre-administration of RTA-404 in *Nfe2l2*^{ENDO} mice.

Fig.4. Endothelial cell Nrf2 maintains microglial homeostatic signature and regulates microglial activation under inflammatory conditions

Mice were given i.p. injection of either saline or RTA-404 (n=6-8) daily for 4 days, following which either saline or LPS was given for 24 hrs. The brain cells were isolated and then sorted with FACS for microglia, RNA extracted and RNA-seq performed. Scatterplot was generated for genes with average expression >0.1 FPKM across the data sets. Highlighted with red and blue crosses are the genes whose expression are significantly increased or decreased respectively (*DESeq2 P*_adj<0.05, n=6-8).

(A) Scatterplot of RNA-seq analysis showing the microglia transcriptome modified by peripheral LPS insult compared with saline in *Nfe2l2*$^{fl/fl}$ mice (LPS vs Saline).

(B) Scatterplot of RNA-seq analysis showing the LPS-induced microglia transcriptome modified by pre-administration of RTA-404 in *Nfe2l2*$^{fl/fl}$ mice (LPS+RTA-404 vs. LPS+saline).

(C) Scatterplot of RNA-seq analysis showing the LPS-induced microglia transcriptome modified by pre-administration of RTA-404 in *Nfe2l2*^{ENDO} mice.

(D) RTA-404 promotes microglial homeostatic signature under inflammatory conditions**.** Genes considered are those expressed >0.5 FPKM in our data and within the group of microglia signature genes defined by (Butovsky et al., 2014). For each gene, $\log_2$ fold change ($\log_2$FC) of microglia gene expression in *Nfe2l2*$^{fl/fl}$ mice by pre-administration of RTA-404 under conditions of LPS exposure (LPS+RTA-404 vs. LPS+saline) is shown. The data were mined from the complete set shown in (B). *P<0.0001, F(1, 498)=95.1 relates to main effect of pre-administration of RTA-404 on microglia signature gene expression under inflammatory conditions, two-way ANOVA.

(E) IPA analysis identifying activated or inhibited pathways in microglia by pre-administration of RTA-404 under conditions of LPS exposure (LPS+RTA-404 vs. LPS+saline). Significantly DEGs (*DESeq2 P*_adj<0.05, $|\text{Log}_2\text{FC}|$>1, n=6-8) with microglia transcriptome as reference dataset were analyzed to calculate the p-value of overlap and z-score of overall activation/inhibition states of individual pathways. The significant activated (p<0.05, z-score >2) or inhibited (p<0.05, z-score <-2) pathways are shown in the bar chart in orange and blue respectively.

(F) The influence of RTA-404 on LPS-induced genes in microglia. For LPS-induced genes (x-axis, FPKM>1*, DESeqP*_adj<0.05, Log_2FC>1) in microglia in *Nfe2l2*$^{fl/fl}$ mice, the Log_2FC (y-axis) of each gene following treatment with LPS ± RTA-404 in microglia in either *Nfe2l2*$^{fl/fl}$ mice or *Nfe2l2*^{ENDO} mice were plotted. (iii) *p=0.0014, F (1,6720) =10.24 relates to main effect of RTA-404 on microglial gene sets induced by LPS, 2-way ANOVA.

(G) The influence of RTA-404 on LPS-repressed genes in microglia. For LPS-repressed genes (x-axis, FPKM>1*, DESeqP*_adj<0.05, Log_2FC <-1) in microglia in *Nfe2l2*$^{fl/fl}$ mice, the log2 fold change (y-axis) of each gene following treatment with LPS ± RTA-404 in microglia in either *Nfe2l2*$^{fl/fl}$ mice or *Nfe2l2*^{ENDO} mice were plotted. (iii): *P<0.0001, F (1,2072) =20.12 relates to main effect of RTA-404 on microglial gene sets suppressed by LPS, 2-way ANOVA.

Fig.5. Endothelial cell Nrf2 is a key point of regulating astrogliosis under inflammatory conditions

Mice were given i.p. injection of either saline or RTA-404 (n=6-8) daily for 4 days, following which either saline or LPS was given for 24 hrs. The brain cells were isolated and then sorted with FACS for astrocytes, RNA extracted and RNA-seq performed. Scatterplot was generated for genes with average

expression >0.1 FPKM across the data sets. Highlighted with red and blue crosses are the genes whose expression are significantly increased or decreased respectively (*DESeq2 P*_adj<0.05, n=6-8).

(A) Scatterplot of RNA-seq analysis showing the astrocyte transcriptome modified by peripheral LPS insult compared with saline in *Nfe2l2*$^{fl/fl}$ mice (LPS vs Saline).

(B) Scatterplot of RNA-seq analysis showing the LPS-induced astrocyte transcriptome modified by pre-administration of RTA-404 in *Nfe2l2*$^{fl/fl}$ mice (LPS+RTA-404 vs. LPS+saline).

(C) Scatterplot of RNA-seq analysis showing the LPS-induced astrocyte transcriptome modified by pre-administration of RTA-404 in *Nfe2l2*^{ENDO} mice**.**

(E) IPA analysis identifying activated or inhibited pathways in astrocytes by pre-administration of RTA-404 under conditions of LPS exposure (LPS+RTA-404 vs. LPS+saline). Significantly DEGs (*DESeq2 P*_adj<0.05, $|Log_2FC|$>1, n=6-8) with astrocyte transcriptome as reference dataset were analyzed to calculate the p-value of overlap and z-score of overall activation/inhibition states of individual pathways. The significantly inhibited (p<0.05, z-score <-2) pathways are shown in the bar chart in blue.

(E) The influence of RTA-404 on LPS-induced genes in astrocytes. For LPS-induced genes (x-axis, FPKM>1*, DESeqP*_adj<0.05, Log_2FC >1) in astrocytes in *Nfe2l2*$^{fl/fl}$ mice, the Log_2FC (y-axis) of each gene following treatment with LPS ± RTA-404 in astrocytes in either *Nfe2l2*$^{fl/fl}$ mice or *Nfe2l2*^{ENDO} mice were plotted. (iii) *p<0.0001, F (1,6056) =29.29 relates to main effect of RTA-404 on astrocytic gene sets induced by LPS, 2-way ANOVA.

(F) The influence of RTA-404 on LPS-repressed genes in astrocytes. For LPS-repressed genes (x-axis, FPKM>1*, DESeqP*_adj<0.05, Log_2FC <-1) in astrocytes in *Nfe2l2*$^{fl/fl}$ mice, the Log_2FC (y-axis) of each gene following treatment with LPS ± RTA-404 in astrocytes in either *Nfe2l2*$^{fl/fl}$ mice or *Nfe2l2*^{ENDO} mice were plotted. (iii): *p<0.0001, F (1,25556) =68.12 relates to main effect of RTA-404 on astrocytic gene sets suppressed by LPS, 2-way ANOVA.

Fig.6. Endothelial cell Nrf2 regulates immune cell brain infiltration under inflammatory conditions

Mice were given i.p. injection of either saline or RTA-404 (n=6-8) daily for 4 days, following which either saline or LPS was given for 24 hrs. The brain cells were analyzed using flow cytometer and the number of macrophages ($CD11b^{+}CD45^{high}$) in the brain following LPS or RTA-404 treatment were quantified.

(A) Representative flow cytometry graphs showing microglia and macrophage population in the brain.

(B) Statistical analysis showing the effect of either LPS or RTA-404 on peripheral monocyte brain infiltration. p=0.0023, 0.0010, 0.0045,0.4774 from left to right, 2-way ANOVA plus Sidak post hoc (n=6-8).

Fig. S1. FACS gating strategy for BECs, astrocytes, microglia and macrophages

(A) Representative flow cytometry graphs are shown for gating strategy for populations of BECs ($CD31^{+}CD45^{-}$), astrocytes ($ACSA2^{+}O4^{-}$), microglia ($CD11b^{+}CD45^{low}$) and macrophages ($CD11b^{+}CD45^{high}$). Brain cells were isolated as single cell suspension from WT mice and labelled with full panel of antibodies for BECs, astrocytes, microglia and macrophages.

(B) Representative flow cytometry graphs are shown for establishing gating strategy for microglia ($CD11b^{+}CD45^{low}$) and macrophages ($CD11b^{+}CD45^{high}$). 1. Brain cells from WT mice without antibody labelling. 2 & 3. Brain cells from *Csf1r*$^{\Delta FIRE/\Delta FIRE}$ mice (2) and WT mice (3) labelled with a panel of antibodies for BECs, astrocytes, microglia and macrophages.

Figure 1

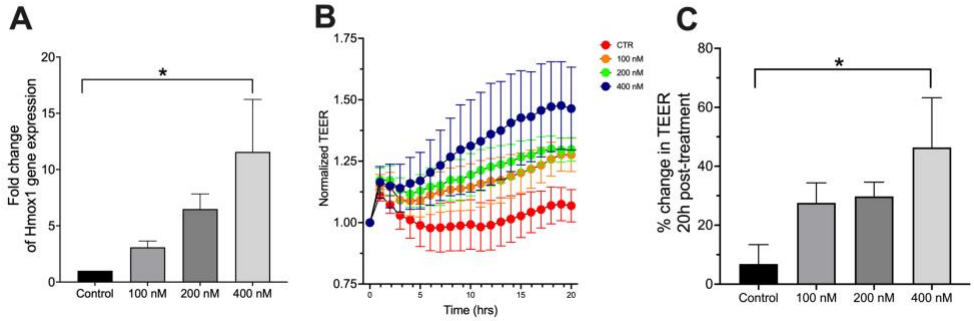

Figure 2

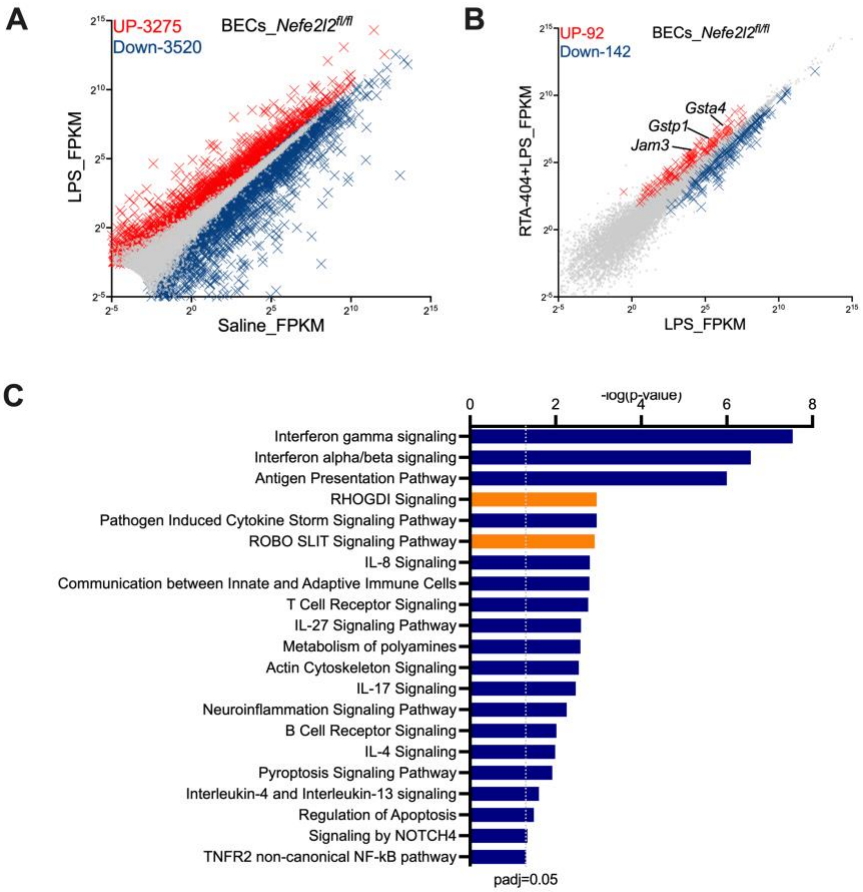

Figure 3

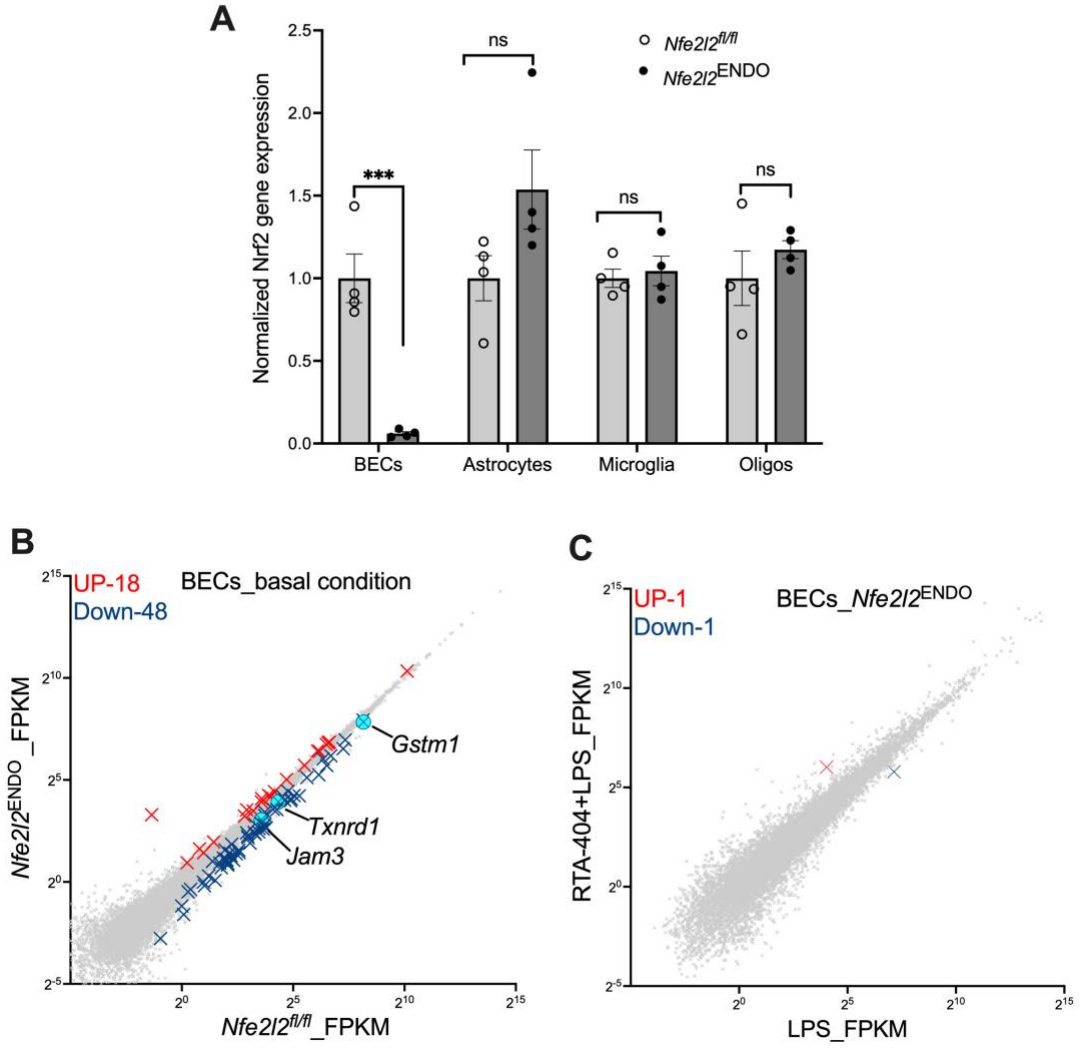
A
Normalized Nrf2 gene expression
2.5
2.0
1.5
1.0
0.5
0.0
***
ns
ns
ns
Nfe2l2fl/fl
Nfe2l2ENDO
BECs
Astrocytes
Microglia
Oligos
B
UP-18
Down-48
BECs_basal condition
Gstm1
Txnrd1
Jam3
Nfe2l2ENDO_FPKM
Nfe2l2fl/fl_FPKM
C
UP-1
Down-1
BECs_Nfe2l2ENDO
RTA-404+LPS_FPKM
LPS_FPKM

Figure 4

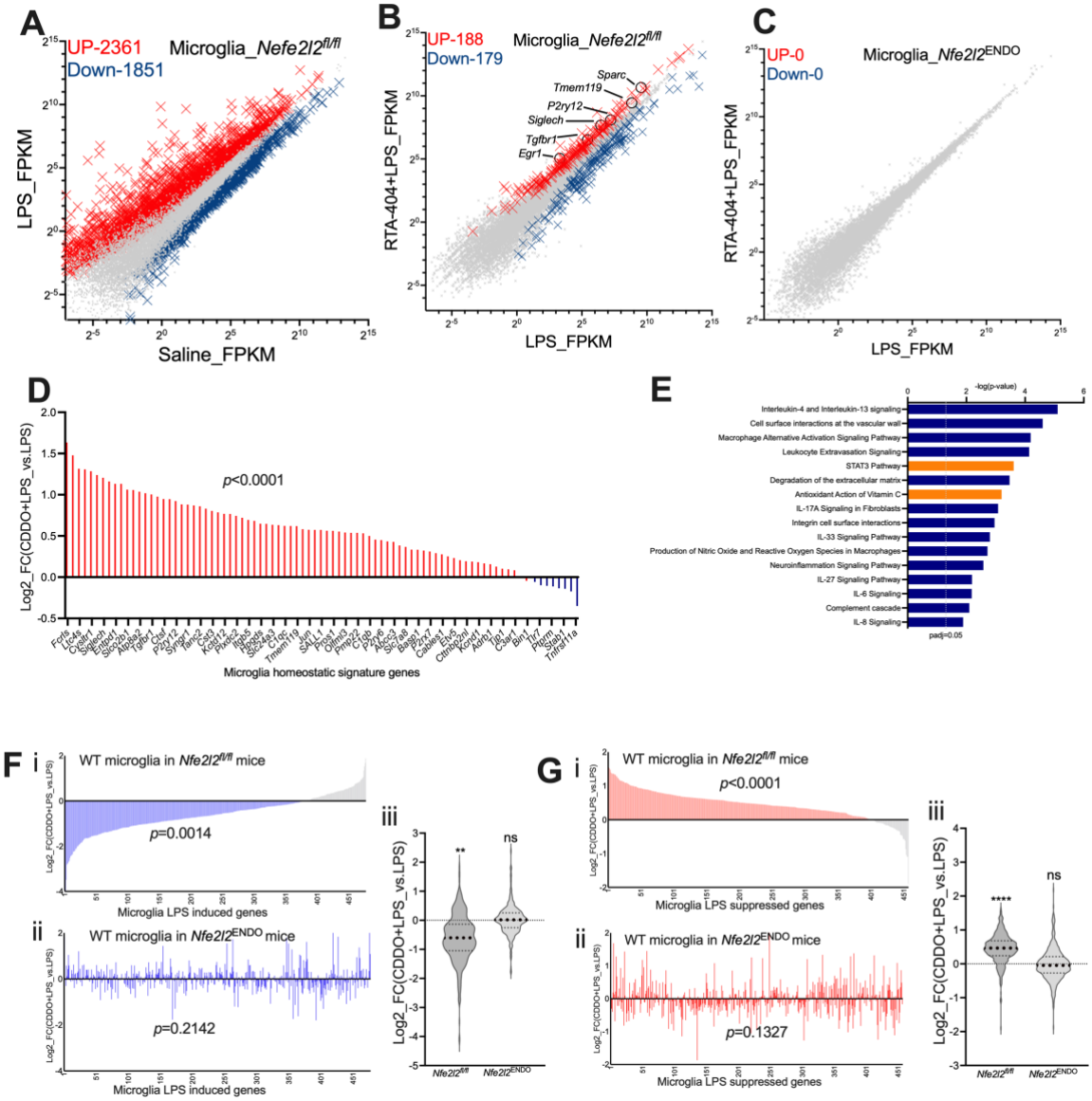
A
UP-2361
Down-1851
Microglia_Nefe2l2fl/fl
LPS_FPKM
Saline_FPKM
B
UP-188
Down-179
Microglia_Nefe2l2fl/fl
Sparc
Tmem119
P2ry12
Siglech
Tgfbr1
Egr1
RTA-404+LPS_FPKM
LPS_FPKM
C
UP-0
Down-0
Microglia_Nfe2l2ENDO
RTA-404+LPS_FPKM
LPS_FPKM
D
p<0.0001
Log2_FC(CDDO+LPS_vs.LPS)
Microglia homeostatic signature genes
E
-log(p-value)
Interleukin-4 and Interleukin-13 signaling
Cell surface interactions at the vascular wall
Macrophage Alternative Activation Signaling Pathway
Leukocyte Extravasation Signaling
STAT3 Pathway
Degradation of the extracellular matrix
Antioxidant Action of Vitamin C
IL-17A Signaling in Fibroblasts
Integrin cell surface interactions
IL-33 Signaling Pathway
Production of Nitric Oxide and Reactive Oxygen Species in Macrophages
Neuroinflammation Signaling Pathway
IL-27 Signaling Pathway
IL-6 Signaling
Complement cascade
IL-8 Signaling
padj=0.05
F
i
WT microglia in Nfe2l2fl/fl mice
p=0.0014
Microglia LPS induced genes
ii
WT microglia in Nfe2l2ENDO mice
p=0.2142
Microglia LPS induced genes
iii
**
ns
Log2_FC(CDDO+LPS_vs.LPS)
Nfe2l2fl/fl
Nfe2l2ENDO
G
i
WT microglia in Nfe2l2fl/fl mice
p<0.0001
Microglia LPS suppressed genes
ii
WT microglia in Nfe2l2ENDO mice
p=0.1327
Microglia LPS suppressed genes
iii
****
ns
Log2_FC(CDDO+LPS_vs.LPS)
Nfe2l2fl/fl
Nfe2l2ENDO

Figure 5

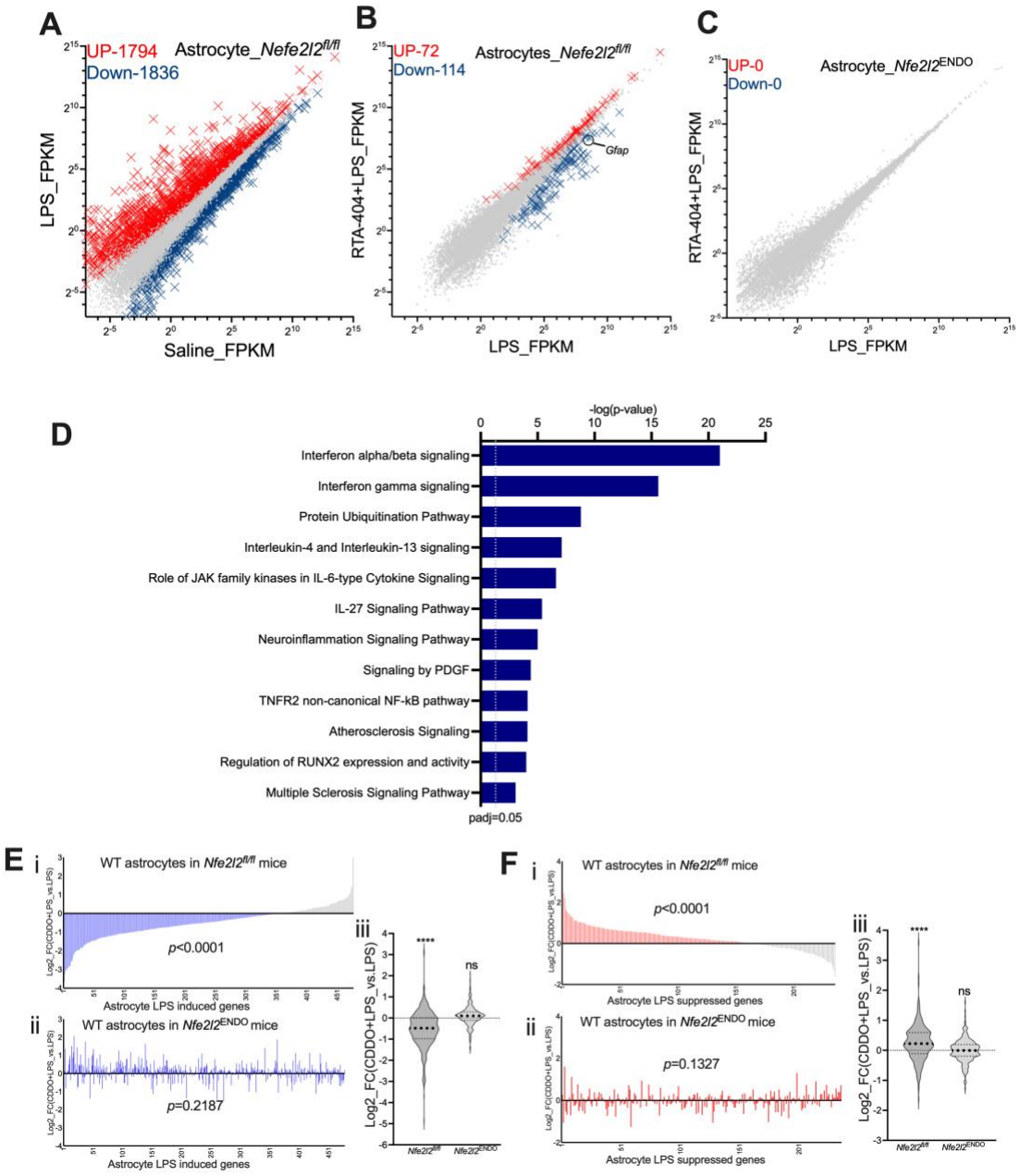
A
UP-1794
Down-1836
Astrocyte_Nefe2l2fl/fl
LPS_FPKM
Saline_FPKM
B
UP-72
Down-114
Astrocytes_Nefe2l2fl/fl
Gfap
RTA-404+LPS_FPKM
LPS_FPKM
C
UP-0
Down-0
Astrocyte_Nfe2l2ENDO
RTA-404+LPS_FPKM
LPS_FPKM
D
-log(p-value)
Interferon alpha/beta signaling
Interferon gamma signaling
Protein Ubiquitination Pathway
Interleukin-4 and Interleukin-13 signaling
Role of JAK family kinases in IL-6-type Cytokine Signaling
IL-27 Signaling Pathway
Neuroinflammation Signaling Pathway
Signaling by PDGF
TNFR2 non-canonical NF-kB pathway
Atherosclerosis Signaling
Regulation of RUNX2 expression and activity
Multiple Sclerosis Signaling Pathway
padj=0.05
E
i
WT astrocytes in Nfe2l2fl/fl mice
p<0.0001
Astrocyte LPS induced genes
ii
WT astrocytes in Nfe2l2ENDO mice
p=0.2187
Astrocyte LPS induced genes
iii
Log2_FC(CDDO+LPS_vs.LPS)
****
ns
Nfe2l2fl/fl
Nfe2l2ENDO
F
i
WT astrocytes in Nfe2l2fl/fl mice
p<0.0001
Astrocyte LPS suppressed genes
ii
WT astrocytes in Nfe2l2ENDO mice
p=0.1327
Astrocyte LPS suppressed genes
iii
Log2_FC(CDDO+LPS_vs.LPS)
****
ns
Nfe2l2fl/fl
Nfe2l2ENDO

Figure 6

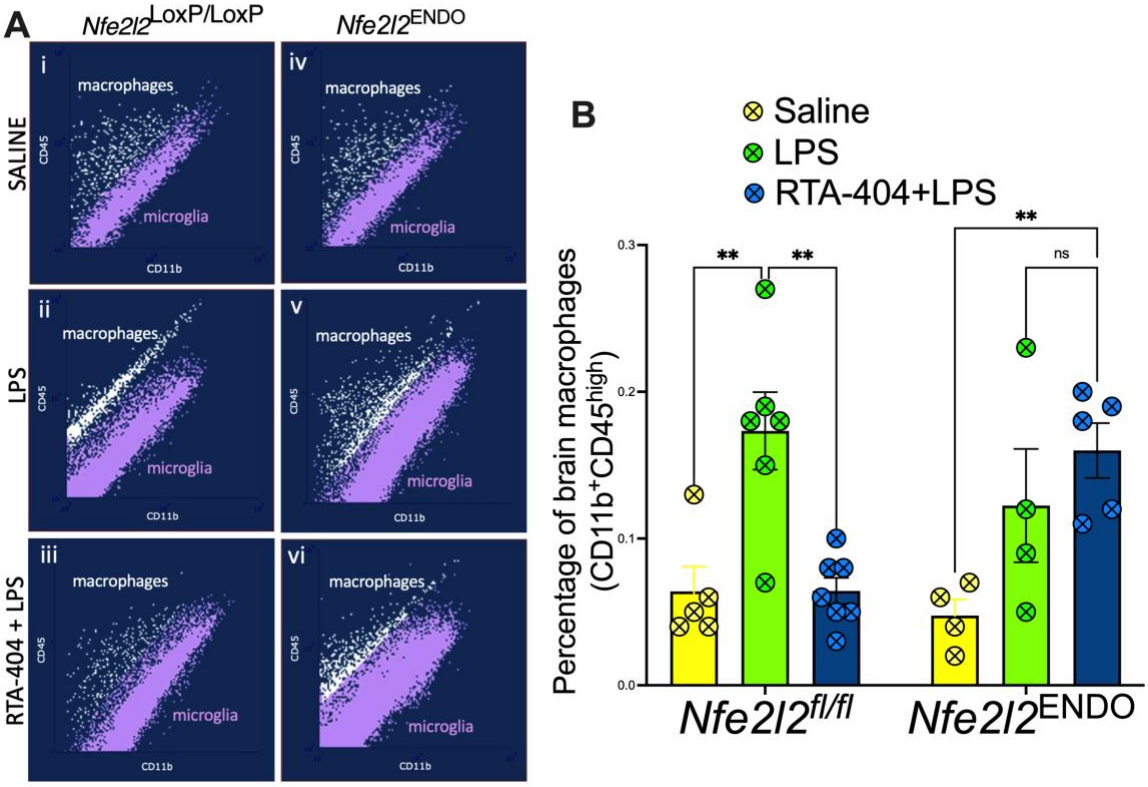
A
Nfe2l2LoxP/LoxP
Nfe2l2ENDO
SALINE
LPS
RTA-404 + LPS
i
ii
iii
iv
v
vi
macrophages
microglia
CD45
CD11b
B
Saline
LPS
RTA-404+LPS
Percentage of brain macrophages (CD11b+CD45high)
0.3
0.2
0.1
0.0
**
**
**
ns
Nfe2l2fl/fl
Nfe2l2ENDO

Figure S1

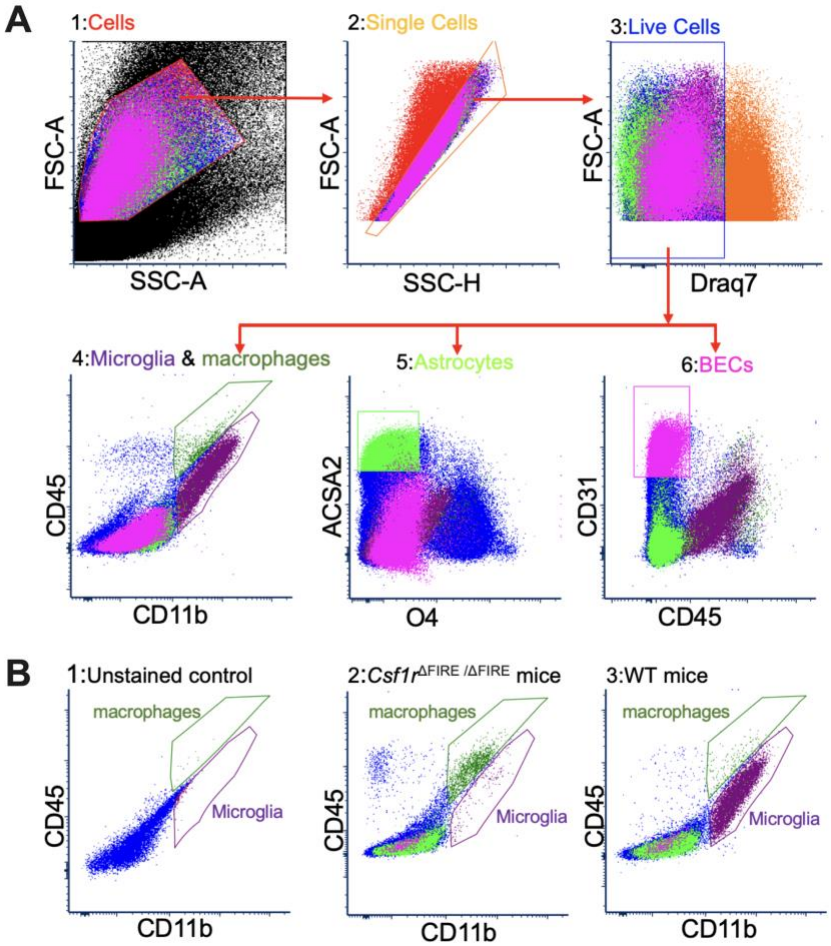
A
1:Cells
FSC-A
SSC-A
2:Single Cells
FSC-A
SSC-H
3:Live Cells
FSC-A
Draq7
4:Microglia & macrophages
CD45
CD11b
5:Astrocytes
ACSA2
O4
6:BECs
CD31
CD45
B
1:Unstained control
macrophages
Microglia
CD45
CD11b
2:Csf1r ΔFIRE /ΔFIRE mice
macrophages
Microglia
CD45
CD11b
3:WT mice
macrophages
Microglia
CD45
CD11b